






ISSN: 1813-162X (Print); 2312-7589 (Online)

Tikrit Journal of Engineering Sciences

available online at: <http://www.tj-es.com>
**TJES**  
 Tikrit Journal of  
 Engineering Sciences

# Simulation of Heat Gain by Conduction Through Walls for Residential Buildings in Iraq: Ramadi City as Case Study

 Kafel A. Mohammed <sup>\*a</sup>, Salah F. A. Sharif <sup>b</sup>, Tareq H. Abed <sup>a</sup>
<sup>a</sup> Renewable Energy Research Centre, University of Anbar, Anbar, Iraq.<sup>b</sup> Air Conditioning and Refrigeration department, Engineering Technology College, Al-Kitab University, Kirkuk. Iraq.

## Keywords:

Building thermal estimation; Cooling load; Building wall materials; Conductive heat transfer; Heat gain; Solar air temperature.

## Highlights:

- Fourier series in MATLAB modelled wall heat gain; type 3 wall reduced gain by 71%.
- Insulated wall (Type 3) cut heat gain by up to 80% vs. other constructions.
- Simulation of 4 wall types in Ramadi showed 1.2% variance from published data.

## ARTICLE INFO

### Article history:

|                          |         |      |
|--------------------------|---------|------|
| Received                 | 05 May  | 2024 |
| Received in revised form | 29 Aug. | 2024 |
| Accepted                 | 20 Oct. | 2024 |
| Final Proofreading       | 25 Aug. | 2025 |
| Available online         | 29 Aug. | 2025 |

© THIS IS AN OPEN ACCESS ARTICLE UNDER THE CC BY LICENSE. <http://creativecommons.org/licenses/by/4.0/>



**Citation:** Mohammed KA, Sharif SFA, Abed TH. Simulation of Heat Gain by Conduction Through Walls for Residential Buildings in Iraq: Ramadi City as Case Study. *Tikrit Journal of Engineering Sciences* 2025; 32(4): 2175.

<http://doi.org/10.25130/tjes.32.4.10>

### \*Corresponding author:

**Kafel A. Mohammed**

Renewable Energy Research Centre, University of Anbar, Anbar, Iraq.



**Abstract:** To accurately estimate the cooling or heating load of a building, it is necessary to calculate the heat gained through the walls under specific climatic conditions. Many effective techniques to perform this task have been developed in the engineering literature, highlighting the importance of selecting sustainable building materials. In this study, the Fourier series, a third harmonic technique, was used in MATLAB to model the heat gain. The simulation process was based on hourly gain fluctuation through the walls, and conductive heat transfer was calculated. This method facilitated the determination of the amount of heat gained through different wall configurations. Input data for the simulation program included the number of layers of walls, as well as the thermal properties of each layer. Area-specific weather information is essential as the calculation is based on solar air temperature. The study was conducted in August 2023 over 24 hours in the City of Ramadi in Iraq. The results showed 1.2% higher than published research. The results showed that the third type of wall was the best. The third type improved the reduction of heat gain by 71% compared to the first type, by 80% compared to the second type, and by 68% compared to the fourth type.

# محاكاة اكتساب الحرارة بالتوصيل الحراري من خلال جدران المباني السكنية في العراق: مدينة الرمادي كدراسة حالة

غافل عزيز محمد<sup>1</sup>، صلاح فرحان<sup>2</sup>، طارق حمد عبد<sup>1</sup>

<sup>1</sup> مركز أبحاث الطاقة المتجددة، جامعة الأنبار / الرمادي - العراق.

<sup>2</sup> قسم التكييف والتبريد/ كلية الهندسة والتكنولوجيا/ جامعة الكتاب / التون كوبري - العراق.

## الخلاصة

لتقدير حمل التبريد أو التدفئة للمبنى بدقة، من الضروري حساب الحرارة المكتسبة عبر الجدران تحت ظروف مناخية محددة. تم تطوير العديد من التقنيات الفعالة لأداء هذه المهمة في الأدبيات الهندسية، مما يسلط الضوء على أهمية اختيار مواد البناء المستدامة. في هذه الدراسة، تم استخدام متسلسلة فورييه، كتنقنية للمعالج التوافقي الثالث، في برنامج MATLAB لنمذجة اكتساب الحرارة. اعتمدت عملية المحاكاة على التقلب الساعي لاكتساب الحرارة عبر الجدران، وتم حساب انتقال الحرارة بالتوصيل. وقد سهلت هذه الطريقة تحديد كمية الحرارة المكتسبة عبر تركيبات جدران مختلفة. تضمنت بيانات الإدخال لبرنامج المحاكاة عدد طبقات الجدران، إلى جانب الخصائص الحرارية لكل طبقة. وتعد معلومات الطقس الخاصة بالموقع ضرورية حيث أن الحساب يعتمد على درجة حرارة الهواء الشمسية. أجريت الدراسة في آب/أغسطس 2023 على مدى 24 ساعة في مدينة الرمادي في العراق. وأظهرت النتائج فرقاً قدره 1,2% أعلى من البحث المنشور. كما أظهرت النتائج أن النوع الثالث من الجدران كان الأفضل. حيث قام النوع الثالث بتحسين تقليل اكتساب الحرارة بنسبة 71% مقارنة بالنوع الأول، وبنسبة 80% مقارنة بالنوع الثاني، وبنسبة 68% مقارنة بالنوع الرابع.

**الكلمات الدالة:** التقدير الحراري للمباني؛ حمل التبريد؛ مواد جدران المباني؛ انتقال الحرارة بالتوصيل؛ اكتساب الحرارة؛ درجة حرارة الهواء الشمسية.

## 1. INTRODUCTION

Iraq's high temperatures have a significant effect on how well buildings perform thermally, particularly in the summer. This increase in temperature also causes a significant amount of electrical energy to be consumed continuously, especially in light of the country's recent population growth. The researchers investigated the benefits of each strategy, with a particular interest in techniques that reduce consumption. The study's objectives were to either employ novel approaches to positive building design, select buildings with beneficial orientations, and utilize clean energies to reduce waste, or to enhance the building's thermal performance by minimizing heat gain or preventing heat transfer to the structure. Examples of these approaches included the use of thermal insulators and building materials with high thermal resistance. The total heat absorbed through the building's walls, which includes heat from outside air and solar radiation, is known as the heat gain from the walls. This gain is determined based on the temperature difference across the wall [1,2]. Thus, the wall heat transmission coefficient is utilized to assess the amount of heat received through a wall. The building envelope, particularly the walls, plays a crucial role in regulating the internal thermal conditions of a space by interacting with the external environment throughout the day. This article aims to conduct a detailed analysis, using simplified simulation techniques, to assess the impact of various factors, such as thermal properties, density, and solar heat gain, on the thermal performance and energy efficiency of opaque walls in tropical climates during summer and winter. The study also evaluates the thermal efficiency of different wall materials and designs to determine the best options for the specific environmental conditions. Additionally, the research

establishes a parametric simulation framework and compares the thermal behavior of materials in response to moderate external temperatures, with a focus on energy conservation. While the methodology provides valuable insights for initial studies, it acknowledges the complexity of predicting the energy consumption of entire buildings. It emphasizes the need for a comprehensive evaluation of wall materials to achieve optimal thermal efficiency [3,4]. When phase change materials (PCM) are included in a building, a substantial thermal barrier is formed between the interior thermal environment and the external environment. This barrier typically results in summertime overheating. To solve this issue, the PCM incorporates an airflow-based Dynamic Insulation System (DIS) to create a composite structure with switchable thermal resistance. Based on the phase transition of the PCM and the heat transfer between the PCM and the circulating air, a theoretical model was constructed by Ref. [5]. The outcome suggested that induced air turbulence and natural convection might both alter thermal resistance. The forced turbulence state achieved the lowest thermal resistance methodically, with closed states and natural convection following. The phase change and temperature contours showed that air could improve temperature uniformity and phase transition distribution. Heat transfer between air and PCM was facilitated by the greater cavity and bigger H/L ratio of the PCM, which resulted in denser airflow. Dis-PCM Early PCM melting and a rapid heat transfer rate were produced by a device with a significant input heat flux or a low flow rate. The multi-layer hollow wall component was then fitted with the integrated DIS-PCM module to confirm its possible use in reducing building overheating. The DIS-PCM module lowered the average

interior wall temperature and increased the pace at which heat was dissipated from the internal thermal environment [6]. External walls and roofs in hot, tropical areas receive solar radiation, absorb some of it, and transmit heat, which makes up a significant portion of the interior environment. Heat is typically lost to the outer environment in colder climates, which can again lead to thermal discomfort. The thermal energy demand is raised in each scenario. These explanations explain why several researchers have devoted themselves to researching methods for improving the thermal efficiency of ceilings and walls. Among the most practical methods is using PCM as a filler with thermal insulation. It adds to the component's thermal inertia without adding much weight and at a reasonably modest cost. Rewriting the one-dimensional pure conduction is the foundation of the PCM composite wall problem. Models of exterior PCM walls and roofing can be found in hot, tropical areas. A moving PCM mesh is included in the numerical solution. To remove grid size impacts, the computational grid has been adjusted. To handle the roof issue, the model was expanded [7]. The main reason for the discrepancy in thermal reaction times is between old and new construction. As a result, the study examined the relationship between the change in indoor air temperature and the thermal response times of historical and contemporary wall systems. The thermal response times of gas concrete and brick wall structures with the same overall heat transfer coefficient were compared, considering the environmental conditions of Kocaeli Province. The temperature fluctuations in the indoor environment, walls, and insulation materials were studied. The insulation thickness of the three distinct building materials was estimated for U values of 0.6, 0.4, and 0.2 W/m<sup>2</sup> K. Moreover, the maximum and minimum amplitudes of indoor air temperature were measured as 0.59 °C and 0.18 °C [8]. The analysis of the wall and the roof is the same. The U-value of the composite construction, along with the interior and outdoor temperatures, determines the basic transmission of heat loss throughout the winter. The connection may be summarized as in Ref. [9].

## 2. LITERATURE SURVEY

After conducting a thorough review of the literature, various strategies and techniques were used throughout the building project life cycle. Multiple case examples were provided to illustrate these techniques. The framework outlined in the text aims to help design teams maintain a proper balance between social, economic, and environmental concerns. It also seeks to change the way construction industry experts evaluate project data, ultimately supporting the sustainability of the building sector [10, 11]. Moreover, the study notes that

the length of summer in Iraq has recently increased, resulting in higher temperatures and increased cooling loads within buildings. To combat harsh weather and achieve acceptable levels of thermal comfort, it is recommended to utilize renewable energy sources and insulation measures in the building envelope [12]. Building envelopes can benefit from the application of a useful technology called latent heat storage in phase change materials (PCM) [13]. The application of a PCM on the wall has successfully shifted the building's space cooling loads. During the night, the heat absorbed by the PCM during the day is released, shifting the cooling burden to the night. As a result, a novel form-stabilized PCM ventilated roof (VRFP) was suggested in this study. To expel the heat from the PCM's solidification and store cooling energy in the roof, cold night air can be used for ventilation during the summer. The ventilation duct is positioned in the intermediate layer, and the stabilized PCM is placed on the top layer. As a result, the temperature inside the surface of this upper layer is somewhat lower than with traditional methods [14,15]. Another approach to solving this type of problem is by utilizing green roofs in Antananarivo, Madagascar. The temperature changes on the upper surface of the building are reduced by 28°C. Studies have been conducted on how green roofs impact indoor air temperature and energy usage [16]. The presence of vegetation decreases the maximum indoor air temperature, which enhances the building's thermal comfort in the summer. The minimum indoor air temperature remains unaffected; however, it can be increased with greater floor thickness. Additionally, a global sensitivity analysis has been conducted on the proposal. This model identifies the main factors that influence energy consumption without considering specific weather data [17,18]. A complex finite Fourier transform (CFFT) approach can be used to analytically solve the heat transfer issue in multi-layer walls with periodic boundary constraints. The process involves transforming the transient heat transfer problem into a dimensionless form and then calculating the temperature at the inner surface of the walls and the hourly change in heat flux into the space from the walls. Additionally, computer software is developed based on the analytical model to perform numerical computations for various multi-layer wall structures found in Turkish buildings. This technique is advantageous as it allows for calculations to be conducted for different climatic conditions, such as varying ambient air temperatures and solar heat inputs, making the CFFT technique a compelling alternative to other analytical and numerical methods [19-21]. The analysis of the wall and the roof is the same as depicted in Fig. 1. The U-value of the composite construction

and the interior and outdoor temperatures determine the basic transmission of heat loss throughout the winter. The connection may be summarized as in [22, 23]  $Q_{(winter)} = U \times A \times (T_i - T_o)$ , where  $T_i$  is the inside air temperature, and  $T_o$  is the outside air temperature.

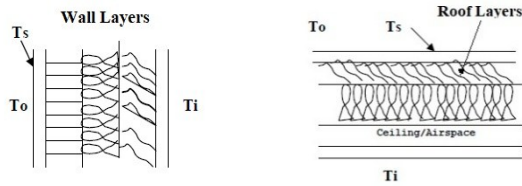


**Fig. 1** Wall and Roof Composite Construction.

Summertime solar radiation impacts the exterior surfaces of walls and roofs. The exterior surface temperature rises as a result of the absorbed radiation to a level higher than that of the surrounding air. Sol-air temperature is the term for the exterior surface temperature [24]. It depends on the characteristics of the roof and wall structures, the material and color of the outside surface, and the component of solar radiation intensity that is perpendicular to the exterior surface. The surface orientation, solar azimuth angle, and solar altitude angle all affect how much solar radiation there is [25, 26]. An approximate formula for the solar-air temperature ( $T_s$ ) of the exterior surface of a given wall or roof is  $T_s = T_o + A \times (I_d + I_s) / H_{so}$ , where  $A$  is the absorption coefficient of outside surface,  $I_d$  is the direct solar radiation on the surface,  $I_s$  is the scatter or diffuse solar radiation, and  $H_{so}$  is the outside wall or roof surface film resistance. The heat gain through a wall or roof in summer is  $Q_{(summer)} = U \times A \times (T_s - T_i)$ . From a review of previous literature, it was noted that many researchers calculated the effects of different temperature variations on different days. In the present study, a theoretical and comparative analysis was conducted in relation to previous research. In the present study, the MATLAB program was used to calculate the heat gain and temperature variation through different walls, for each wall according to its composition. In this study, heat gain effect lines were used on three walls. The temperature lines and streamlines were extracted to obtain a deep understanding of the effect of heat gain on the walls.

### 3. MODELLING FORMATION

Based on the transmission matrix approach, a computer model has been constructed to simulate heat transfer out of walls and roofs. Using a transmission matrix as a reference, the transmission matrix approach connects the cyclic temperature and heat flux on one side of a homogeneous layer to the cyclic temperature and heat flux on the other side [1]:

$$\begin{bmatrix} t_o \\ q_o \end{bmatrix} = \begin{bmatrix} A & B \\ C & D \end{bmatrix} \begin{bmatrix} t_i \\ q_i \end{bmatrix} \quad (1)$$

where  $t_i$  is the inside temperature of the layer (K),  $t_o$  is the outside surface temperature of the

layer (K),  $q_i$  is the inside heat flux ( $W/m^2$ ), and  $q_o$  is the outside heat flux ( $W/m^2$ ). The complex matrix elements  $A$ ,  $B$ ,  $C$ , and  $D$  are based on the thermal features of the layer, as follows [27]:

$$A = \cosh F(L + L_j) \quad (2)$$

$$B = \sinh F(L + L_j) / k(F + F_j) \quad (3)$$

$$C = k(F + F_j) \sinh F(L + L_j) \quad (4)$$

$$D = A \quad (5)$$

$$F = (w/2a)^{1/2} \quad (6)$$

$$a = k / \rho c_p \quad (7)$$

where  $L$  is the slab thickness (m),  $a$  is the thermal diffusivity ( $m^2/sec$ ),  $w$  is the harmonic frequency (1/sec),  $\rho$  is the density ( $kg/m^3$ ),  $c_p$  is the specific heat ( $J/kg.K$ ), and  $k$  is the thermal conductivity ( $W/m.K$ ). The total transmission matrix for each wall is achieved by chain multiplying the individual matrices in the order the matrices are shown in the composite wall section from outside to inside [28]:

$$\begin{bmatrix} A & B \\ C & D \end{bmatrix} = \begin{bmatrix} A1 & B1 \\ C1 & D1 \end{bmatrix} \begin{bmatrix} A2 & B2 \\ C2 & D2 \end{bmatrix} \dots \begin{bmatrix} Ak & Bk \\ Ck & Dk \end{bmatrix} \quad (8)$$

where  $k$  is the number of harmonics.

Generally, the temperature is represented in the complex form of a Fourier series expression as [29]:

$$t = \bar{t}_o + \sum T_i \exp(j\phi_i) \quad (9)$$

where  $\bar{t}_o$  is the average sol-air temperature through 24 hours. The exponential coefficient  $T$  and phase lag  $\Phi$  for each harmonic  $n$  are calculated as [26]:

$$T_n = (M_n^2 + N_n^2)^{1/2} \quad (10)$$

$$\Phi_n = \tan^{-1}(-N_n/M_n) \quad (11)$$

where  $M_n$  and  $N_n$  are the Fourier coefficients that are calculated, as presented in Table 1. For the first, second, and third harmonics. Table 1 presents the values of the Fourier coefficients for wall type one, as an example. The steady-state portion of heat flux is simply calculated as [27]:

$$\bar{q} = \frac{\Delta t}{R} \quad (12)$$

where  $\Delta t$  is the average temperature differential across the layer (K), and  $R$  is the thermal resistance of the layer ( $m^2.K/W$ ). The complete inside heat flux for  $n$  harmonics is achieved by summation or superimposing the steady-state and transient portions as [28]:

$$q_i = \bar{q}_i + \sum_{k=1}^n q_{ik} \quad (13)$$

Equation (13) can be used for computing either the inside or outside heat flux. In the sophisticated simulation model, the transient inside and outside air temperatures are described in the complex form of a Fourier series expression [28]. The inside and outside ( $t$ s) and ( $q$ s) then point to the situations inside the building and the outside ambient conditions. The surface air film resistances are addressed as additional layers of the composite

layer; the transmission matrix elements for a resistance air film are [29]:

$$A = 1, B = 1/h, C = 0, \text{ and } D = 1$$

where  $h$  is the surface heat transfer coefficient ( $\text{W}/\text{m}^2\cdot\text{K}$ ). When calculating the heat flow through several materials (multi-layer), the total transmission matrix is the product of the transmission matrix for each material in the order in which it appears in the composite layer [30]. Assuming the transmission matrix demonstrated in Eq. (3) to be the aggregate transmission matrix for a composite wall section and that the inside and outside air temperatures are known, one can solve for  $q_i$ . The transient heat flux on the inside of the building is [31]:

$$q_i = \frac{t_o}{B} - \left(\frac{A}{B}\right)t_i \quad (14)$$

For the distinct case when the inside-air temperature stays constant over time,  $t_i = 0$  in Eq. (14). Then, the transient heat flux on the inside of the building is expressed merely as [32]:

$$q_i = \frac{t_o}{B} \quad (15)$$

The impact of solar radiation on the heat gains or losses of building sections can be documented by using the sol-air temperatures for each wall orientation, as outside ambient air temperature [33]. A MATLAB computer program was developed to determine the heat gain using the transmission matrix method. The Fourier series third harmonic was implemented, and its results are tabulated in Table 1. The simulation's calculation depends on the composite constructions of the walls, as well as the roofs and the sol-air temperature.

**Table 1** Fourier Series Analysis for Outside Sol–Air Temperature.

| Time   | $t_o$ (°F) | $w_1\theta$                     | $t_o\cos w_1\theta$ | $t_o\sin w_1\theta$ | $w_2\theta$ | $t_o\cos w_2\theta$         | $t_o\sin w_2\theta$ | $w_3\theta$ | $t_o\cos w_3\theta$ | $t_o\sin w_3\theta$         |  |
|--------|------------|---------------------------------|---------------------|---------------------|-------------|-----------------------------|---------------------|-------------|---------------------|-----------------------------|--|
| 1 A.M. | 86         | 15                              | 83.0696             | 22.2584             | 30          | 74.4782                     | 43.0000             | 60          | 43.0000             | 74.4782                     |  |
| 2      | 84         | 30                              | 72.7461             | 42.0000             | 60          | 42.0000                     | 72.7461             | 120         | -42.0000            | 72.7461                     |  |
| 3      | 81         | 45                              | 57.2756             | 57.2756             | 90          | 0.0000                      | 81.0000             | 180         | -81.0000            | 0.0000                      |  |
| 4      | 79         | 60                              | 39.5000             | 68.4160             | 120         | -39.5000                    | 68.4160             | 240         | -39.5000            | -68.4160                    |  |
| 5      | 78         | 75                              | 20.1879             | 75.3422             | 150         | -67.5500                    | 39.0000             | 300         | 39.0000             | -67.5500                    |  |
| 6      | 81         | 90                              | 0.0000              | 81.0000             | 180         | -81.0000                    | 0.0000              | 360         | 81.0000             | -0.0000                     |  |
| 7      | 83         | 105                             | -21.4820            | 80.1718             | 210         | -71.8801                    | -41.5000            | 60          | 41.5000             | 71.8801                     |  |
| 8      | 95         | 120                             | -47.5000            | 82.2724             | 240         | -47.5000                    | -82.2724            | 120         | -47.5000            | 82.2724                     |  |
| 9      | 107        | 135                             | -75.6604            | 75.6604             | 270         | -0.0000                     | -107.0000           | 180         | -107.0000           | 0.0000                      |  |
| 10     | 117        | 150                             | -101.325            | 58.5000             | 300         | 58.5000                     | -101.325            | 240         | -58.5000            | -101.325                    |  |
| 11     | 126        | 165                             | -121.7067           | 32.6112             | 330         | 109.1192                    | -63.0000            | 300         | 63.0000             | -109.119                    |  |
| 12     | 131        | 180                             | -131.000            | 0.0000              | 360         | 131.0000                    | -0.0000             | 360         | 131.0000            | -0.0000                     |  |
| 1 P.M. | 133        | 195                             | -128.4681           | -34.423             | 30          | 115.1814                    | 66.5000             | 60          | 66.5000             | 115.1814                    |  |
| 2      | 131        | 210                             | -113.4493           | -65.500             | 60          | 65.5000                     | 113.4493            | 120         | -65.5000            | 113.4493                    |  |
| 3      | 125        | 225                             | -88.3883            | -88.3883            | 90          | 0.0000                      | 125.0000            | 180         | -125.000            | 0.0000                      |  |
| 4      | 117        | 240                             | -58.5000            | -101.325            | 120         | -58.5000                    | 101.3250            | 240         | -58.5000            | -101.320                    |  |
| 5      | 106        | 255                             | -27.4348            | -102.388            | 150         | -91.7987                    | 53.0000             | 300         | 53.0000             | -91.7987                    |  |
| 6      | 103        | 270                             | -0.0000             | -103.000            | 180         | -103.000                    | 0.0000              | 360         | 103.0000            | -0.0000                     |  |
| 7      | 97         | 285                             | 25.1054             | -93.6948            | 210         | -84.0045                    | -48.5000            | 60          | 48.5000             | 84.0045                     |  |
| 8      | 93         | 300                             | 46.5000             | -80.5404            | 240         | -46.5000                    | -80.5404            | 120         | -46.5000            | 80.5404                     |  |
| 9      | 88         | 315                             | 62.2254             | -62.2254            | 270         | -0.0000                     | -88.0000            | 180         | -88.0000            | 0.0000                      |  |
| 10     | 84         | 330                             | 72.7461             | -42.0000            | 300         | 42.0000                     | -72.7461            | 240         | -42.0000            | -72.7461                    |  |
| 11     | 80         | 345                             | 77.2741             | -20.7055            | 330         | 69.2820                     | -40.0000            | 300         | 40.0000             | -69.2820                    |  |
| 12     | 77         | 360                             | 77.000              | -0.0000             | 360         | 77.0000                     | -0.0000             | 360         | 77.0000             | -0.0000                     |  |
| Sum    | 2382       |                                 | -281.284            | -118.682            |             | 92.827                      | 41.462              |             | -14.5               | 13.08                       |  |
|        |            | $\bar{t}_0 = 2382 / 24 = 99.25$ |                     |                     |             | $M_2 = 92.872 / 12 = 7.735$ |                     |             |                     | $M_3 = -14.5 / 12 = -1.208$ |  |
|        |            | $M_1 = -281.284 / 12 = -23.44$  |                     |                     |             | $N_2 = 41.462 / 12 = 3.455$ |                     |             |                     | $N_3 = 13.08 / 12 = 1.090$  |  |
|        |            | $N_1 = -118.682 / 12 = -9.89$   |                     |                     |             |                             |                     |             |                     |                             |  |

Table 1 displays the Fourier series analysis of solar and outdoor air temperature, which is crucial for understanding heat gain through walls. Fourier series analysis is a mathematical technique used to represent periodic functions, such as the sum of sine and cosine functions. In the context of this study, the external temperature of the sun and the air show periodic variations, and the Fourier series helps break down these variations into harmonics for further examination.

• **Columns:**

- 1- **Solar time** indicates the time of day in solar time format.
- 2-  **$w_3\theta$ ,  $w_2\theta$ ,  $w_1\theta$** : These bars stand for the relative angular frequencies of the second, third, and first harmonic

components. To determine if temperature fluctuations are cyclical, it is necessary to conduct such studies.

- 3-  **$t_o\cos(w_3\theta)$ ,  $t_o\sin(w_3\theta)$** : The fourth harmonic cosine and sine components are given by these columns, which help within the Fourier

- 4-  **$t_o\cos(w_2\theta)$ ,  $t_o\sin(w_2\theta)$** : These columns, just like the ones sometime recently, appear the moment harmonic's cosine and sine components.

• **Explanation:**

- Angular frequencies ( $w_3$ ,  $w_2$ ,  $w_1$ ): These numbers demonstrate particular cycles at different temperatures and build up the swaying speed for each consonant.

• Cosine and sine components: Each harmonic's cosine and sine values demonstrate the stage and size of the related temperature alteration.

• Normal discuss and sun-based temperature (up to):

The thermal properties of the layers used in the present study are illustrated in [Table 2](#).

**Table 2** Constructions of Wall Types.

| Type of wall | Construction                       | Thickness (m) | Thermal Conductivity (W/m.K) | Density (kg/m <sup>3</sup> ) |
|--------------|------------------------------------|---------------|------------------------------|------------------------------|
| Type One     | -Cement Plaster                    | 0.025         | 0.717                        | 1858                         |
|              | -Common Brick                      | 0.2           | 0.725                        | 1922                         |
|              | -Gypsum or another similar layer   | 0.02          | 0.752                        | 1601                         |
| Type Two     | -Face Brick                        | 0.1           | 1.344                        | 2082                         |
|              | -Ordinary Concrete Block           | 0.2           | 0.1.07                       | 977                          |
|              | -Gypsum or other similar finishing | 0.02          | 0.752                        | 1061                         |
| Type Three   | -Cement Plaster                    | 0.025         | 0.717                        | 1858                         |
|              | -Face Brick                        | 0.1           | 1.344                        | 2082                         |
|              | -Insulation                        | 0.05          | 0.044                        | 91                           |
| Type Four    | -Ordinary Concrete Block           | 0.2           | 1.075                        | 977                          |
|              | -Gypsum or other similar finishing | 0.02          | 0.752                        | 1061                         |
|              | -Cement Plaster                    | 0.025         | 0.717                        | 1858                         |
| Type Four    | -Concrete Block                    | 0.2           | 1.075                        | 977                          |
|              | -Gypsum or other similar finishing | 0.02          | 0.752                        | 1061                         |

[Table 2](#) provides important details about the composition and characteristics of materials used in constructing different types of walls. It includes information on the density, thickness, and thermal conductivity of each layer of each type of wall. These characteristics vary depending on the layers and materials used.

• **Columns:**

- 1- The **wall type** depicts how walls are separated into four particular classifications: Type 1, Type 2, Type 3, and Type 4.
- 2- **Construction:** Traces the materials and layers used to construct each kind of wall.
- 3- **Thickness (m):** This demonstrates each layer's thickness in meters.
- 4- **The capacity of a substance to transfer heat** is decided by its heat conductivity, which is communicated in Watts per Kelvin times meter (W/m.K).
- 5- **Density:** This metric, which is communicated in kilograms per cubic meter (kg/m<sup>3</sup>), portrays the mass of each fabric per unit volume.

• **Explanation:**

- **Wall Type:** Makes a difference in recognizing certain engineering properties by clearly separating different wall types.
- **Construction** depicts the layers and materials required to make each sort of wall.
- **Thickness:** Builds up the thickness of each layer, which is crucial for comprehending the wall's basic components.
- **Thermal conductivity:** Demonstrates how well a material conducts heat, which affects the overall sum of heat exchanged through walls.
- **Density:** The amount of materials per unit volume decides the walls' general weight and basic characteristics.

An illustration to understand the first type:

• **Construction:** The first type of wall consisted of layers of cement plaster, common brick, plaster, or a similar layer.

• **Thickness:** The cement plaster layer was 0.025 m, the common brick layer was 0.2 m, and the plaster layer was 0.02 m.

• **Thermal conductivity:** Cement plaster has a thermal conductivity of 0.717 W/m.K, ordinary brick has a thermal conductivity of 0.725 W/m.K, and gypsum has a thermal conductivity of 0.752 W/m.K.

• **Density:** Its density is 1858 kg/m<sup>3</sup> for cement plaster, 1922 kg/m<sup>3</sup> for common brick, and 1601 kg/m<sup>3</sup> for plaster.

This table serves as a crucial reference to understand the composition of different types of walls, as it provides basic data to analyze their thermal and structural properties in the context of the study.

#### 4.RESULTS AND DISCUSSIONS

The simulation study concentrated on calculating the heat gain through walls in the City of Ramadi. It utilized the Fourier series and the third harmonic technique, as implemented by the MATLAB program. The research aims to provide valuable insights into the variations in heat gain between different types of walls and configurations under specific climatic conditions.

##### 4.1.Methodology of the Simulation

Using cutting-edge MATLAB software, the simulation includes hourly heat gain estimates based on 24-hour solar air temperature in August 2023. The study examined several wall types and configurations, each with its structure and set of warm characteristics.

**Examination of wall types:** Four walls with varying insulating qualities and compositions were examined in the present study:

- 1- **The first type:** cement plaster, ordinary bricks, and plaster.
- 2- **The second type:** regular concrete blocks, facing bricks, and plaster.

- 3- **The third type:** face bricks, cement plaster, plaster, regular concrete blocks, and insulation.
- 4- **Fourth type:** cement plaster, concrete block, and plaster.

#### **Important outcomes:**

**Distinctive types of walls give distinctive amounts of heat gain.** The tapes on the wall have a significant impact on the warmth received, which varies throughout the day.

- 1- **The third wall:** centers on how materials influence heat execution and consolidates cover, which had the smallest amount of heat gain.
- 2- **Insulation's effect on heat gain:** The separator, especially in wall 3, essentially diminished heat gain, highlighting the requirement of utilizing well-insulated and economically developed materials to reduce heat transmission.
- 3- **Variety in heat gain over time:** The study found that heat gain varied over time, reaching its highest values at specific hours. Understanding these varieties can improve vitality proficiency strategies and building design.
- 4- **Comparison with published studies about**
  - When the discoveries for the City of Ramadi were compared to past

pondering, they showed a 1.2% rise in temperature [25].

- This distinction highlights the need for region-specific contemplations in building plans and can be attributed to neighborhood climate circumstances.

#### **4.2. Results for Sustainable Building**

The study provides valuable information about effective construction methods, particularly for dry regions. The findings emphasize the importance of choosing the proper insulation and construction materials to reduce heat gain, save energy costs, and improve overall building efficiency.

#### **4.3. Restrictions and Future Directions**

Even though they consider offering smart data, it is essential to note that it has several limitations.

- The simulation's capacity to be broadly connected is constrained since it is considered for a certain time period and a set of climate factors.
- Future studies ought to study other factors for a more exhaustive examination, such as ventilation, shading, and real-time meteorological information.

**Table 3** compares the heat gain obtained through simulation for various wall types over specific time periods. To comprehend how different wall structures perform in terms of heat gain under various daytime scenarios, an understanding of the data is necessary.

**Table 3** Comparison of Results Obtained by Simulation.

| Time   | Heat Gain, W/m <sup>2</sup><br>(Wall type One) | Heat Gain, W/m <sup>2</sup><br>(Wall type Two) | Heat Gain, W/m <sup>2</sup><br>(Wall type Three) | Heat Gain, W/m <sup>2</sup><br>(Wall type Four) |
|--------|--|--|--|---|
| 1 A.M. | 30.4675  | 37.7603  | 10.8465  | 27.7614   |
| 2      | 24.0287  | 31.5196  | 10.1472  | 21.9005   |
| 3      | 20.4975  | 26.1921  | 9.3631   | 18.1008   |
| 4      | 20.1146  | 22.1409  | 8.5479   | 16.6213   |
| 5      | 22.9061  | 19.642   | 7.7569   | 17.5627   |
| 6      | 28.6817  | 18.8658  | 7.0441   | 20.861  |
| 7      | 37.0478  | 19.8652  | 6.4581   | 26.2914   |
| 8      | 47.4344  | 22.5721  | 6.0389   | 33.4838   |
| 9      | 59.1335  | 26.8019  | 5.8149   | 41.948  |
| 10     | 71.3479  | 32.2664  | 5.8015   | 51.1072   |
| 11     | 83.2451  | 38.5933  | 5.9995   | 60.3372   |
| 12     | 94.0145  | 45.3513  | 6.3956   | 69.009  |
| 1 P.M. | 102.922  | 52.08  | 6.9626   | 76.5317   |
| 2      | 109.361  | 58.3207  | 7.6619   | 82.3925   |
| 3      | 112.892  | 63.6481  | 8.4459   | 86.1922   |
| 4      | 113.275  | 67.6993  | 9.2612   | 87.6716   |
| 5      | 110.483  | 70.1981  | 10.0522  | 86.7301   |
| 6      | 104.708  | 70.9742  | 10.765   | 83.4317   |
| 7      | 96.3413  | 69.9748  | 11.3509  | 78.0013   |
| 8      | 85.9547  | 67.2679  | 11.7702  | 70.8089   |
| 9      | 74.2556  | 63.038   | 11.9942  | 62.3447   |
| 10     | 62.0412  | 57.5735  | 12.0076  | 53.1854   |
| 11     | 50.1439  | 51.2466  | 11.8095  | 43.9554   |
| 12     | 39.3746  | 44.4885  | 11.4135  | 35.2836   |

#### **• Columns:**

- 1- **Time** depicts multiple times during the day, running from one hour intervals at one in the morning to three in the afternoon to twelve at midnight.
- 2- **Heat Gain, W/m<sup>2</sup> (First Wall Type)** presents the total heat gained

for Wall Type I per square meter over time.

- 3- **Heat gain, W/m<sup>2</sup> (Second wall Type)** presents values of heat gain that match Type II walls.

4- **Heat Gain,  $W/m^2$  (Third Wall Type)** presents the third wall type's heat gain figures.

5- **Heat gain,  $W/m^2$  (Fourth wall type)** presents the fourth wall type's heat gain values.

• **Explanation:**

• **Time** shows precise times of day, making it simple to monitor patterns in temperature rise over time.

• **Heat gain** shows the amount of heat that each kind of wall receives per square meter during the day.

Example of interpretation at 8 A.M.:

• **First type wall:** 47.4344 Watts/ $m^2$

• **Second type Wall:** 22.5721 watts/ $m^2$

• **Third wall type:** 33.4838  $W/m^2$

• **Fourth wall type:** 41.9480  $W/m^2$

The above table provides a thorough understanding of how each type of wall performs in terms of heat gain at different times of the day. Researchers and practitioners can analyze these results to gain insight into the

thermal efficiency of various wall constructions. This information helps in selecting appropriate materials for sustainable building design in a specific context. Figure 2 compares the expected results with the results published by Ismail Kamal [25]. The comparative results showed a small and acceptable percentage, around 1.2%. The simulation was conducted for four types of wall constructions. The results are shown in Figures 3, 4, 5, and 6 for wall types one, two, three, and four, respectively. The results showed the heat gain variation through 24 hours. Figure 7 compares different types of walls during August 2023. It is noted that there was a significant difference in heat gain. This difference indicates the extent to which the type of wall affects the value of heat gain, as heat transfer to the first wall was better and higher than the rest of the walls. The third wall was less valuable due to its construction and the type of wall present, as the first layer was 11 times better than the third layer.

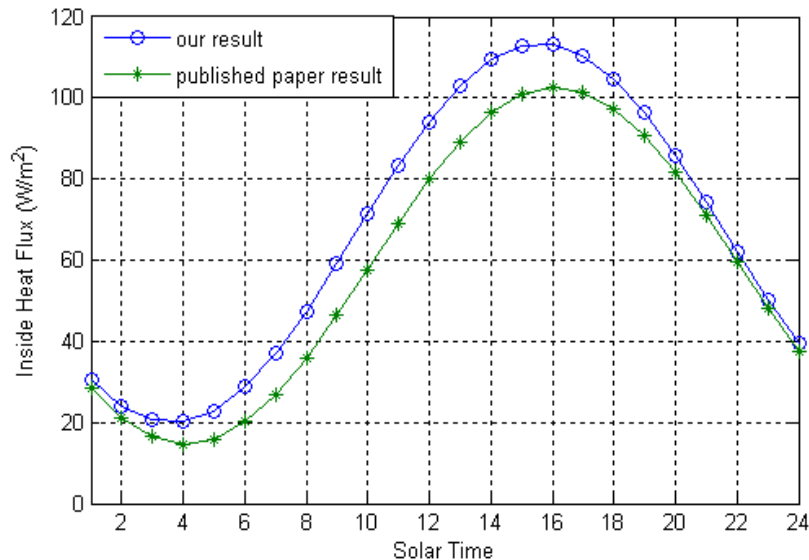


**Fig. 2** Comparison of the Present Results with the Previous Study [25].

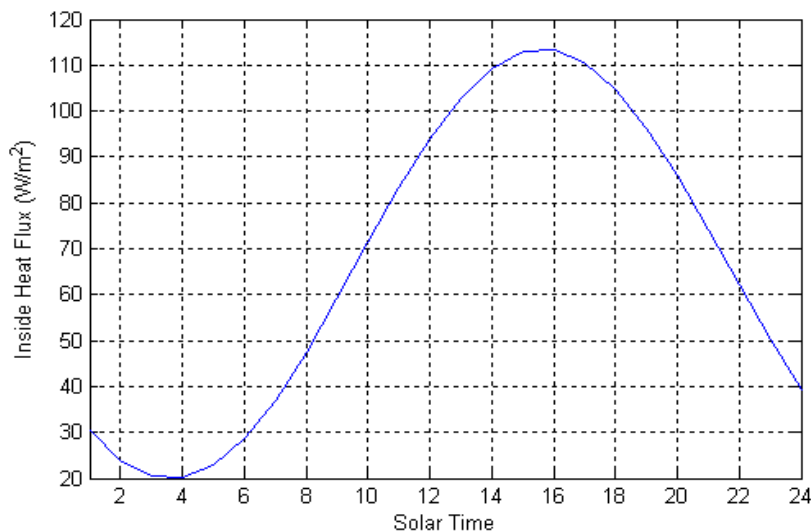


**Fig. 3** Transient Heat Gain by Conduction Through a Wall Section (Wall Type One).



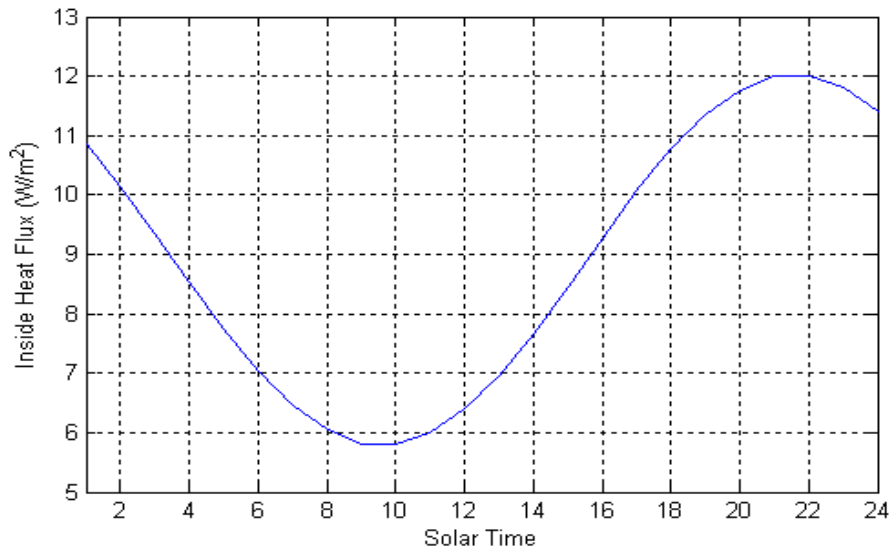


**Fig. 4** Transient Heat Gain by Conduction Through a Wall.

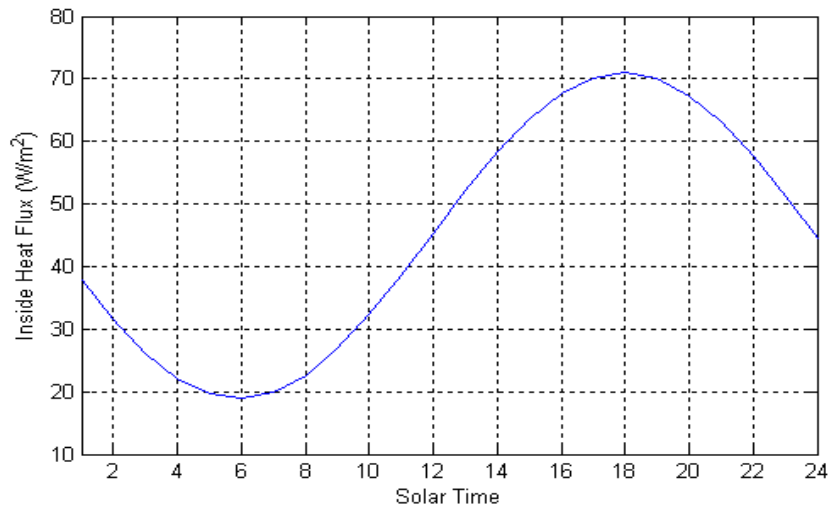


**Fig. 5** Transient Heat Gain by Conduction Through a Wall Section (Wall Type Three).

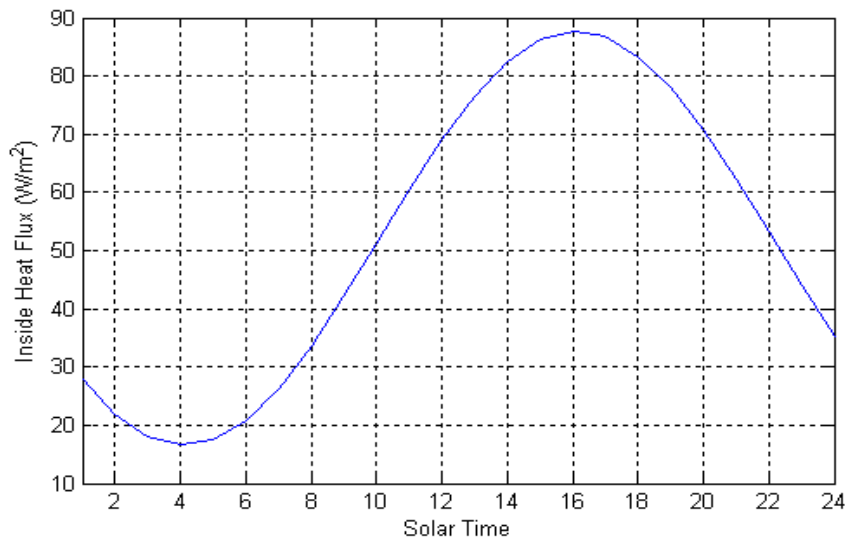


**Fig. 6** Transient Heat Gain by Conduction Through a Wall Section (Wall Type Four).

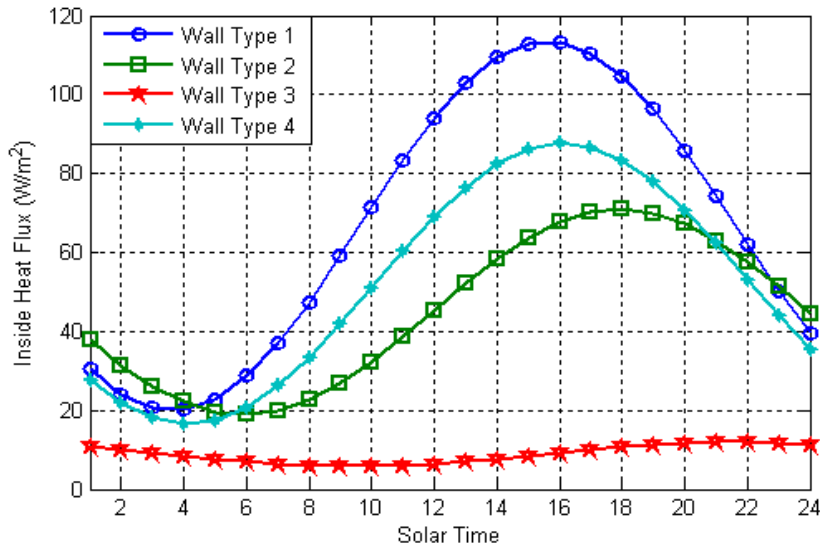


**Fig. 7** Comparison of Transient Heat Gain by Conduction Through the Four Walls.

## 5. CONCLUSIONS

The present work involved creating a computer program to calculate the conduction-based heat transfer from a section of a wall using the transfer matrix approach. Developing this program required advanced knowledge of complex arithmetic methods, prime matrices, and the Fourier series. An advanced analysis method was developed to compute the heat gain using the matrix method within MATLAB. Comparisons with published works demonstrated a high level of agreement, with variances of about 1.2%. This model also offers easy and flexible usability.

- 1) The results indicated the varying effect of wall materials and layers, which can be used to choose the appropriate design for walls and ceilings, depending on the designer's requirements for the value of heat gain (heating or insulation).
- 2) The essential advantage of the transfer matrix technique is the simplicity with which the model can take advantage of transient air temperatures.
- 3) The results during a day in August 2023 indicated a difference in heat gain across three layers. The results showed that the best heat gain was in the first layer. The worst heat gain was in the third layer due to the presence of insulation. The first layer was 11 times better than the third layer. Therefore, the transfer matrix method had the potential to easily document changes in heat gain by conduction that can be achieved by changing the indoor air temperature.
- 4) The findings indicated that the third type of wall was the best. When the study's results were compared, the third type's heat transfer reduction was improved by 71% compared to the first type, 80% compared

to the second type, and 68% compared to the fourth type.

## ACKNOWLEDGEMENTS

The authors are grateful for the financial support towards this research by the Renewable Energy Research Centre, University of Anbar.

## REFERENCES

- [1] Buffington DE. **Heat Gain by Conduction Through Exterior Walls and Roofs.** Transmission Matrix Method; 1975.
- [2] Sharif SF, A'Adel HN, Yaseen AH. **Pre-Pressed and Burnt Sandy Clay Tiles Used to Cover Exposed Concrete Roofs as a Sustainable Alternative.** *Journal of Duhok University* 2020; **23**(2): 278–287.
- [3] Akadiri PO, Chinyio EA, Olomolaiye PO. **Design of a Sustainable Building: A Conceptual Framework for Implementing Sustainability in the Building Sector.** *Buildings* 2012; **2**(2): 126–152.
- [4] Azeez K, Ahmed RI, Obaid ZA, Azzawi ID. **Heat Transfer Enhancement and Applications of Thermal Energy Storage Techniques on Solar Air Collectors: A Review.** *Journal of Thermal Engineering* 2021; **9**(5): 1356–1371.
- [5] Azeez K, Ahmed RI. **Heat Transfer Enhancement for Corrugated Facing Step Channels Using Aluminium Nitride Nanofluid-Numerical Investigation.** *Journal of Thermal Engineering* 2022; **8**(6): 734–747.
- [6] Zhang Z, Zhang N, Yuan Y, Phelan PE, Attia S. **Thermal Performance of a Dynamic Insulation-Phase Change Material System and Its Application**

- in Multilayer Hollow Walls. *Journal of Energy Storage* 2023; **62**: 106912.**
- [7] Ismail KA, Castro JN, Lino FA. **Thermal Insulation of Walls and Roofs by PCM: Modeling and Experimental Validation.** *International Journal of Engineering and Applied Sciences* 2015; **2**(9): 257820.
- [8] Yüksel A, Arıcı M, Karabay H. **Comparison of Thermal Response Times of Historical and Modern Building Wall Materials.** *Journal of Thermal Engineering* 2021; **7**(6): 1506–1518.
- [9] Wetter M. **Simulation-Based Building Energy Optimization.** University of California; 2004.
- [10] Kareem AK, Gabir MM, Almoayed OM, Ismail AE, Taib I, Darlis N, Ali IR. **A Systematic Review on Cardiovascular Stent and Stenting Failure: Coherent Taxonomy, Performance Measures, Motivations, Open Challenges and Recommendations.** *International Journal of Integrated Engineering* 2022; **14**(1): 102–126.
- [11] Al-Damook A, Khalil WH. **Experimental Evaluation of an Unglazed Solar Air Collector for Building Space Heating in Iraq.** *Renewable Energy* 2017; **112**: 498–509.
- [12] Azeez K, Obaid ZA, Their KM. **Investigating the Experimental Parameters of a Rib Triple Pipe Heat Exchanger.** *Case Studies in Thermal Engineering* 2023; **44**: 102859.
- [13] Jannat N, Hussien A, Abdullah B, Cotgrave A. **A Comparative Simulation Study of the Thermal Performances of the Building Envelope Wall Materials in the Tropics.** *Sustainability* 2020; **12**(12): 4892.
- [14] Al-Yasiri Q, Al-Furaiji MA, Alshara AK. **Comparative Study of Building Envelope Cooling Loads in Al-Amarah City, Iraq.** *Journal of Engineering & Technological Sciences* 2019; **51**(5): 654–668.
- [15] Azeez K, Their KM, Ibrahim ZA. **Evaluation of Flat Plate Solar Heater Filling in Nanofluid Under Climatic of Iraq Conditions.** *Case Studies in Thermal Engineering* 2022; **39**: 102447.
- [16] Yu J, Leng K, Wang F, Ye H, Luo Y. **Simulation Study on Dynamic Thermal Performance of a New Ventilated Roof with Form-Stable PCM in Southern China.** *Sustainability* 2020; **12**(22): 9315.
- [17] Rakotondramiarana HT, Ranaivoarisoa TF, Morau D. **Dynamic Simulation of the Green Roofs Impact on Building Energy Performance, Case Study of Antananarivo, Madagascar.** *Buildings* 2015; **5**(2): 497–520.
- [18] Mohsen PS, Pourfayaz F, Shirmohamadi R, Moosavi S, Khalilpoor N. **Potential, Current Status, and Applications of Renewable Energy in Energy Sector of Iran: A Review.** *Renewable Energy Research and Applications* 2021; **2**(1): 25–49.
- [19] Kalogirou SA. **Solar Thermal Collectors and Applications.** *Progress in Energy and Combustion Science* 2004; **30**(3): 231–295.
- [20] Mohammed KA, Saleem AM, Obaid ZA. **Numerical Investigation of Nusselt Number for Nanofluids Flow in an Inclined Cylinder.** *Frontiers in Heat and Mass Transfer* 2021; **16**: 25.
- [21] Yumrutaş R, Ünsal M, Kanoğlu M. **Periodic Solution of Transient Heat Flow Through Multilayer Walls and Flat Roofs by Complex Finite Fourier Transform Technique.** *Building and Environment* 2005; **40**(8): 1117–1125.
- [22] Omle I, Askar AH, Kovács E, Bolló B. **Comparison of the Performance of New and Traditional Numerical Methods for Long-Term Simulations of Heat Transfer in Walls with Thermal Bridges.** *Energies* 2023; **16**(12): 4604.
- [23] Their KM, Azeez K, Mohsin MA. **Thermohydraulic Performance Study of the Effect of Winglet Inserts and a Corrugated Wall in a Rectangular Channel.** *Case Studies in Thermal Engineering* 2023; **52**: 103707.
- [24] Zhang Z, Zhang N, Yuan Y, Phelan PE, Attia S. **Thermal Performance of a Dynamic Insulation-Phase Change Material System and Its Application in Multilayer Hollow Walls.** *Journal of Energy Storage* 2023; **62**: 106912.
- [25] Ismail KA, Castro JN, Lino FA. **Thermal Insulation of Walls and Roofs by PCM: Modeling and Experimental Validation.** *International Journal of Engineering and Applied Sciences* 2015; **2**(9): 257820.
- [26] Yüksel A, Arıcı M, Karabay H. **Comparison of Thermal Response Times of Historical and Modern Building Wall Materials.** *Journal of Thermal Engineering* 2021; **7**(6): 1506–1518.
- [27] Wetter M. **Simulation-Based Building Energy Optimization.** University of California; 2004.
- [28] Kareem AK, Gabir MM, Almoayed OM, Ismail AE, Taib I, Darlis N, Ali IR. **A**

- Systematic Review on Cardiovascular Stent and Stenting Failure: Coherent Taxonomy, Performance Measures, Motivations, Open Challenges and Recommendations.** *International Journal of Integrated Engineering* 2022; **14**(1): 102–126.
- [29] Wepfer WJ. **Application of the Second Law to the Analysis and Design of Energy Systems.** The University of Wisconsin-Madison; 1979.
- [30] Burke K, Finn D, Kenny P. **The Transparency and Repeatability of Building Energy Performance Certification.** Athens, Greece; 2005.
- [31] Obaid ZA, Azzawi ID, Azeez K. **The Experimental Study of Energy Features for Solar Air Heaters with Different Turbulator Configurations.** *Heat Transfer* 2023; **52**(2): 1380–1394.
- [32] Pragati S, Shanthi Priya R, Pradeepa C, Senthil R. **Simulation of the Energy Performance of a Building with Green Roofs and Green Walls in a Tropical Climate.** *Sustainability* 2023; **15**(3): 2006.
- [33] Khalaf KA, Gamil A, Attiya B, Cuello J. **Exploring the Potential of Concentrating Solar Power Technologies for Vertical Farming in Arid Regions: The Case of Western Iraq.** *Energy for Sustainable Development* 2023; **77**: 101310.